BEST AVAILABLE IMAGES

Defective images within this document are accurate representations of the original documents submitted by the applicant.

Defects in the images may include (but are not limited to):

- BLACK BORDERS
- TEXT CUT OFF AT TOP, BOTTOM OR SIDES
- FADED TEXT
- ILLEGIBLE TEXT
- SKEWED/SLANTED IMAGES
- COLORED PHOTOS
- BLACK OR VERY BLACK AND WHITE DARK PHOTOS
- GRAY SCALE DOCUMENTS

IMAGES ARE BEST AVAILABLE COPY.

As rescanning documents *will not* correct images, please do not report the images to the Image Problem Mailbox.

be WO 96/05846
translation (partial).

Example 1

Complete removal of scrapie virus. As a model for so called slow viruses or prions, scrapie virus was bred in a group of hamsters and after spiking administered by 5 serial cartridges on a production typical ultrafiltration plant and the infectivity of the ultrafiltrates examined in an animal test (see figure 1).

1.1 *Obtaining infectious scrapie virus*

A hamster brain infected with scrapie stock+ 263K was macerated and pooled in terminal stage. 500mg of this was added to 4.5ml sterile physiological salt dilution, homogenised and centrifuged for 10 min at 500g. 50µl of the remainder was injected intracerebrally into 40 Syrian LVG-hamsters. The animals were euthanised after this has become necessary due do their clinical state. This took on average 65 to 80 days from the injection. The brains were removed aseptically, frozen, macerated, mixed with a sterile cooking salt dilution and homogenised. Afterwards, they were centrifuged for 10min at 500g and the remainder was used as "spike" material.

1.2 *Obtaining thymus gland homogenate*

Three calves` thymus glands (ca. 550g) were pureed, mixed with 1.5L pyrogen free water and homogenised. The homogenate was stored at 4°C until usage.

The pre-filters and the ultrafilters were washed with water, as usual. For the pre-filtration, thymus extract was filtered through nylon gauze and three microfiltration membranes (Pall, nylon membranes) with pore sizes 2.0µm, 0.8µm and 0.2µm. To ensure that the virus` distance was not falsified through particle absorption on the large inner surface of the spiral cartridges and to measure filtration reduction only, filters were pre-spiked for virus reduction. Pre-filters and filters were pre-treated with the thymus homogenate obtained, i.e. only a small amount (4x 200ml) was passed through the filter at a time.

1.3 *Removal of the scrapie virus*

10ml of the scrapie spike dilution obtained in sample 1 was added to 600ml of the thymus homogenate and stored overnight at 4°C. Then, the dilution was filtered through a first pre-filter with a pore size of 2.0µm, a second pre-filter with a pore size of 0.8µm and a third pre-filter with a pore size of 0.2µm. The filtrate was labelled as Probe A.

190ml of the spiked pre-filtrate material was again mixed with 6ml of the scrapie spike dilution and then ultrafiltered with an Amicon membrane S1Y30. The filtrate was labelled as Probe B.

144ml of Probe B was again mixed with 6ml of the scrapie spike material and ultrafiltered for a second time with another Amicon S1Y30 membrane. The filtrate was labelled as Probe C.

121 ml of Probe C was again mixed with 6ml of the scrapie spike material and again ultrafiltered with the same membrane. The filtrate is labelled was Probe D.

121ml of Probe D was ultrafiltered for a fourth time with the same membrane. The dilution obtained was labelled as Probe E.

93ml of Probe E was ultrafiltered for a fifth time with the same membrane. The dilution obtained is labelled as Probe F.

Probe F subsequently was led via a sterile filtration to a 0.2µm filter. The filtrate obtained is labelled as Probe G.

Figure 1 gives an overview over the method used.

This method gave an infection titre of $10^{8,\ 4\ 5}$ LD50/ml for the starting material. After three pre-filtrations for Probe A $10^{4,\ 9\ 7}$ LD50/ml the total number of infectious virus before the first ultrafiltration after respiking was (6ml x $10^{8,\ 4,\ 5}$) $10^{9,\ 2\ 3}$ LD50 units (150ml). After ultrafiltration, Probe B was given only $10^{4,\ 5\ 6}$ LD50 units ($10^{2,\ 3\ 8}$ LD50/ml). This gives a virus reduction of factor $10^{4,\ 6\ 7}$ at the first ultrafiltration.

Reduction at second ultrafiltration

After respiking the Probe (6ml x $10^{8,\ 4\ 5}$) the dilution (127ml) contained $10^{9,\ 2\ 3}$ virus altogether. The infection titre which was found despite another spiking after the second ultrafiltration was smaller than 1 LD50/ml, i.e. there was no more virus found. This gives a titre in 127ml of $<10^2$ LD50. So the reduction in the second ultrafiltration step is larger than $10^{7,\ 1\ 3}$.

As described previously, Probe G was determined. Here, an reduction factor > $10^{7,\ 2\ 8}$ was found.

Figure 2 shows the reduction data of the scrapie virus through serial ultrafiltration. In contrast to the result theoretically expected, a constant or even decreasing reduction as observed with serial filtration of bacteriophage *fr* over the same ultrafiltration membrane S1Y30 (WO 91/12027, table 3), the reduction rate for the scrapie Virus increases after the second filtration step by more than 2 ten potencies.

Through serial ultrafiltration even the reduction of titre through autoclaving or alkali treatment (both considered as secure) can be fallen short of significantly. That way, you can manufacture a drug without danger potential through virus of spongiform encephalopathies. Independent of this, additional pre or post cleaning steps can of course be combined with this method described. This method distinguished by the Virus being removed through ultrafiltration until the product positively is not infectious any more.

The available experiments prove that with a repetitious ultrafiltration the removal of infectious agents like prions or so called "slow viruses", the reduction speed per filtration step increases at least 100 or 1000fold which leads to a rapid acceleration of virus distance and therefore to an infection security of the product.

Patent Claims

1. Method for the manufacture of pharmaceutical products and/or foods made from material probably contaminated with prions, including the secure removal of the infectious agents: prions only are removed by repetitious filtration through an ultrafiltration membrane and/or a series of ultrafiltration membranes.

2. Method according to one of the previous demands: the infectious material is a virus of spongiform encephalophaty.

3. Method according to one of the previous demands: the virus causes scrapie, BSE, Kuru, Gerstmann-Straeussler, Creutzfeld-Jakob and/or Alzheimer.

4. Method according to one of the previous demands: before use, the filtration membrane is pre-treated with the material to be filtered.

5. Method according to one of the previous demands: from the second ultrafiltration, the virus is removed by at least a factor of 10^{-6}, preferably 10^{-7}.

6. Method according to one of the previous demands: the pharmaceutical product contains thymus fraction, heparin, natural and/or recombinant proteins from cell cultures and/or human growth factor.

7. Method according to one of the previous demands: the pharmaceutical product consists of Interleukin-2, recombinant glyco protein and/or tissue plasminogen activator.

8. Method according to one of the previous demands: as ultrafiltration membrane, an Amicon spiral membrane with tangential flow S1Y30, S10Y30 or S100Y30 is used.

9. Method according to one of the previous demands: the ultrafiltration membrane is validated through spiking with virus of the Leviviridae family.

10. Method according to one of the previous demands: control by means of a pressure test.

Table 1/2

Reduction of scrapie virus via ultrafiltration

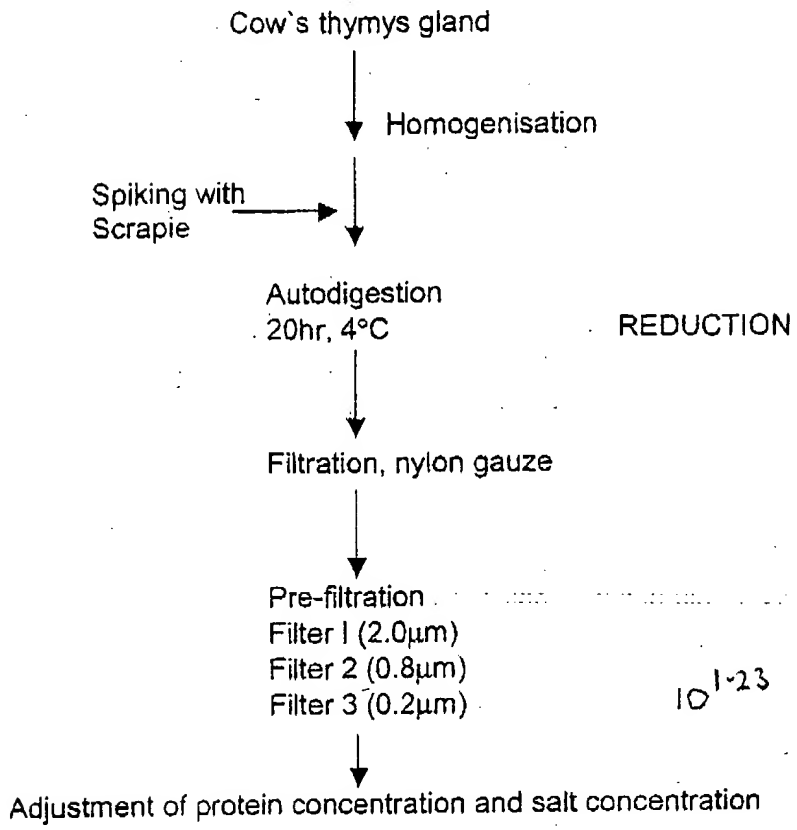

Fig 2:

Reduction of Scrapie virus
By manifold ultrafiltration

Table 1/2

Reduction of scrapie virus via ultrafiltration

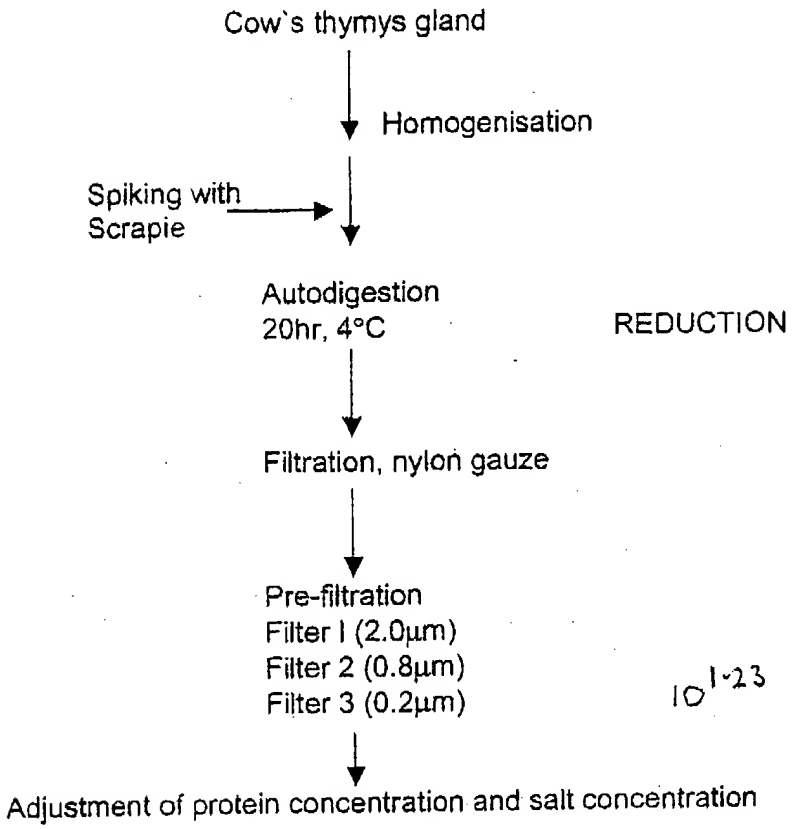

Fig 2:

Reduction of Scrapie virus
By manifold ultrafiltration

PRINCIPLES OF VIROLOGY

Molecular Biology, Pathogenesis, and Control

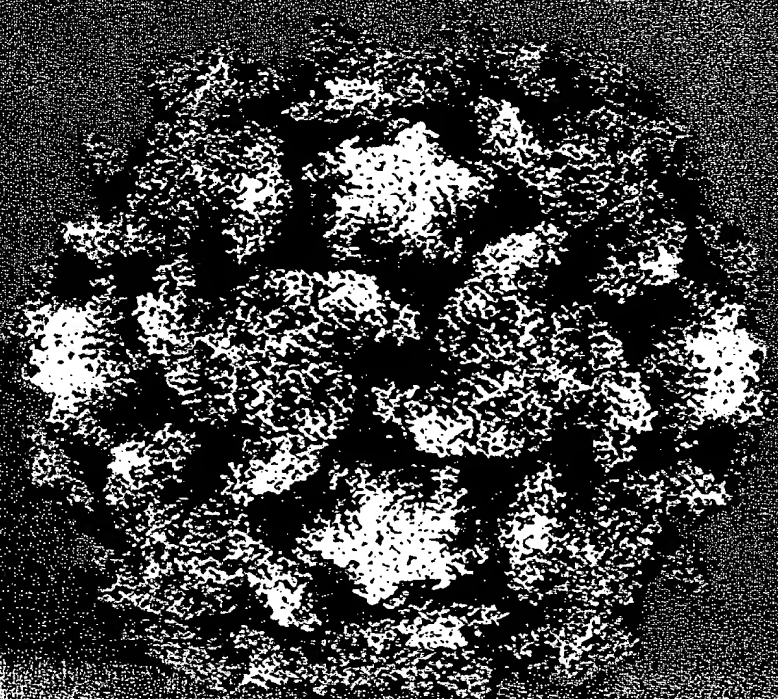

S. J. FLINT
L. W. ENQUIST
R. M. KRUG
V. R. RACANIELLO
A. M. SKALKA

Front cover illustration: A model of the atomic structure of the poliovirus type 1 Mahoney strain. The model has been highlighted by radial depth cuing so that the portions of the model that are farthest from the center are bright. Prominent surface features include a star-shaped mesa at each of the fivefold axes and a propeller-shaped feature at each of the threefold axes. A deep cleft or canyon surrounds the star-shaped feature. This canyon is the receptor-binding site. Courtesy of Robert Grant, Stéphane Crainic, and James Hogle (Harvard Medical School).

Back cover illustration: Progress in the global eradication of poliomyelitis has been striking, as illustrated by maps showing areas of known or probable circulation of wild-type poliovirus in 1988 and 1998. Blue indicates either the presence of virus or insufficient surveillance to exclude the possibility of virus circulation. In 1988, virus was present on all continents except Australia. By 1998, the Americas were free of wild-type poliovirus, and transmission was interrupted in the western Pacific region (including the People's Republic of China) and in the European region (with the exception of southeastern Turkey). There are currently three major foci of transmission: southern Asia (Afghanistan, Pakistan, and India), West Africa (mainly Nigeria), and central Africa (mainly the Democratic Republic of Congo). Source: World Health Organization.

American Society for Microbiology
1752 N Street NW
Washington, DC 20036

Library of Congress Cataloging-in-Publication Data
Principles of virology: molecular biology, pathogenesis, and control / S. J. Flint ... [et al.].
p. cm.
Includes bibliographical references and index.
ISBN 1-55581-127-2 (hardcover)
1. Viruses. 2. Virology. I. Flint, S. Jane.
[DNLM: 1. Viruses. 2. Virology—methods. QW 160 P957 2000]
QR360.P697 2000
579.2—dc21
DNLM/DLC
for Library of Congress
99-14697
CIP

10 9 8 7 6 5 4 3 2

Printed in the United States of America

Illustrations and illustration concepting: J/B Woolsey Associates
Cover and interior design: Susan Brown Schmidler

BOX 1.2

The episome

In 1958, François Jacob and Elie Wollman realized that lambda prophage, the *E. coli* F sex factor, and the colicinogenic factor had many common genetic properties. Their remarkable insight led to the concept of the episome.

An **episome** is an exogenous genetic element not necessary for cell survival. Its defining characteristic is the ability to reproduce in two alternative states by integrating into the host chromosome or by autonomous replication.

Nowadays this term is often applied to genomes that can be maintained in cells by autonomous replication and never integrate, for example, certain viral DNA genomes.

Jacob and Wollman immediately understood that the episome had value in understanding larger problems, including cancer, as revealed by this quotation: "Thus in the no man's land between heredity and infection, between physiology and pathology at the cellular level, episomes provide a new link and a new way of thinking about cellular genetics in bacteria, and perhaps in mice, men and elephants" (F. Jacob and E. Wollman, *Viruses and Genes: Readings from Scientific American* [W. H. Freeman & Co., New York, N.Y., 1961]).

mortal cell lines such as the mouse L and human HeLa cells which are still in widespread use. These advances allowed growth of animal cells in culture to become a routine, reproducible exercise.

The availability of well-characterized cell cultures had several important consequences for virology. It allowed the discovery of several new human viruses, such as adenovirus, measles virus, and rubella virus, for which animal hosts were not available. In 1949 John Enders and colleagues used cell cultures to propagate poliovirus, a feat that led to development of the Sabin vaccine a few years later. Tissue culture technology revolutionized the ability to investigate the replication of viruses in host cells. Viral infectious cycles could be studied under precisely controlled conditions by employing the analog of the one-step growth cycle of bacteriophages and simple methods for quantification of infectious particles. Our current understanding of the molecular basis of parasitism by viruses, the focus of the initial chapters of this book, is based almost entirely on analyses of one-step growth cycles with cells in culture. Such studies established that viruses are **molecular parasites**: they reproduce by exploiting their host cell's biosynthetic machinery for synthesis of the components from which they are built. Thus, in contrast to cells, viruses do not reproduce by growth and division. Rather, the infecting genome contains viral information necessary to redirect cellular systems to the production of all the components needed to assemble new virus particles.

Viruses Defined

Advances in knowledge of the structure of virus particles and the mechanisms by which viruses reproduce in their host cells have been accompanied by increasingly accurate definitions of these unique agents. The earliest, pathogenic, agents, distinguished by their small size and dependence on a host organism for reproduction, emphasized the importance of viruses as agents of disease. We can now provide a much more precise definition of viruses, elaborating their relationship with the host cell and the important features of virus particles. The definitive properties of viruses are summarized as follows:

- A virus is a very small, infectious, obligate intracellular (molecular) parasite.
- The virus genome comprises either DNA or RNA.
- Within an appropriate host cell, the viral genome is replicated and directs the synthesis, by cellular systems, of other virion components.
- Progeny virions are formed by de novo assembly from newly synthesized components within the host cell.
- A progeny virion assembled during the infectious cycle is the vehicle for transmission of the viral genome to the next host cell or organism, where its disassembly leads to the beginning of the next infectious cycle.

With these properties in mind, we can accurately place viruses within the evolutionary continuum of biological agents. They are far simpler than even the smallest microorganisms and lack the complex energy-generating and biosynthetic systems necessary for independent existence. On the other hand, viruses are not the simplest biologically active agents: even the smallest virus, built from a very limited genome and a single type of protein, is significantly more complex than other parasitic molecular

pathogens. Some of these minimalist molecular pathogens, **viroids**, which are infectious agents of a variety of economically important plants, comprise a single small molecule of RNA. Others, termed **prions**, are believed to be single molecules of protein.

Cataloging of Diverse Animal Viruses

Many Sizes and Shapes Produced by Evolution

Around 1960 virus classification was a subject of colorful and quite heated controversy. New viruses were being discovered and studied by electron microscopy. The virus world consisted of a veritable zoo of particles with different sizes, shapes, and compositions (Fig. 1.9). Very strong opinions were advanced concerning classification and nomenclature, and opposing camps developed, as in any controversy involving individuals who tend to focus on differences and those who look for similarities (conventionally known as **splitters** and **lumpers**). Splitters pointed to the inability to infer, from the known properties of viruses, anything about their evolutionary origin or their relationships to one another—the major goal of classical taxonomy. Lumpers maintained that, despite such limitations, there were significant practical advantages in grouping isolates with similar properties. Furthermore, it seemed likely that a good classification might actually stimulate fruitful investigation. A major sticking point, however, was finding agreement on the properties that should be considered most important in constructing a scheme for virus classification.

The Classical System of Classification

In 1962 Lwoff, R. W. Horne, and P. Tournier advanced a comprehensive scheme for the classification of all viruses (bacterial, plant, and animal) under the classical Linnaean hierarchical system consisting of phylum, class, order, family, genus, and species. Although a subsequently formed international committee on the nomenclature of viruses did not adopt this system in toto, many principles embodied in the system were accepted, and its designation of families, genera, and species was used by this committee in the classification of animal viruses.

One of the most important principles embodied in the system advanced by Lwoff and his colleagues was that viruses should be grouped according to *their* shared prop-

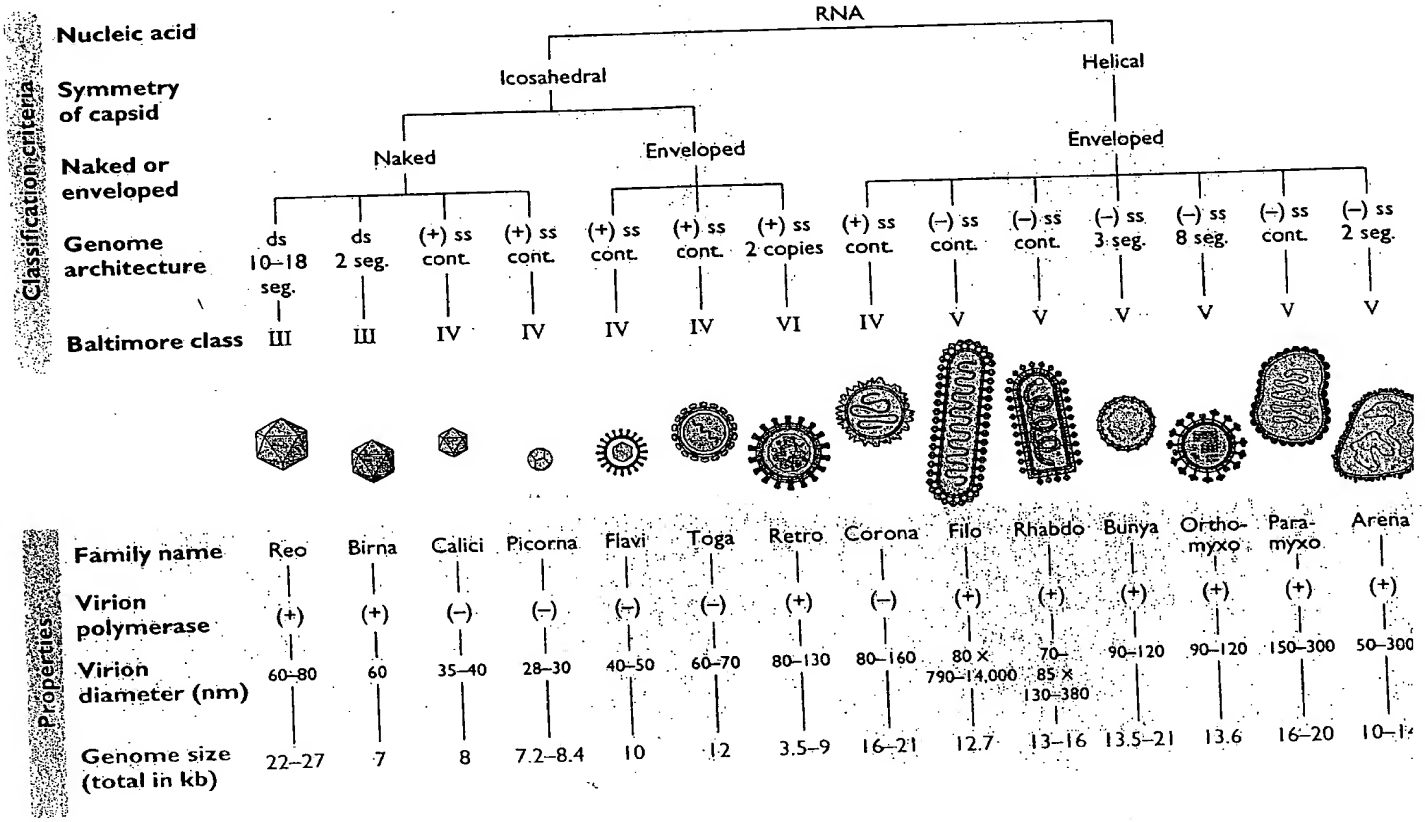

erties rather than the properties of the cells or organisms they infect. A second was a focus on the nucleic acid genome as the primary criterion for classification. The importance of the genome had become clear when it was inferred from the Hershey-Chase experiment that viral nucleic acid alone can be infectious. The system delineated four characteristics to be used in the classification of all viruses:

1. Nature of the nucleic acid in the virion (DNA or RNA)
2. Symmetry of the capsid
3. Presence or absence of an envelope
4. Dimensions of the virion and capsid.

These and a few additional properties are summarized in Fig. 1.9, which lists 21 families of viruses that infect humans and other mammals.

The order in which families are aligned in the figure is arbitrary, as the evolutionary relationships among families are still largely unknown. However, it is clear that the morphological distinctions highlighted in the scheme belie some significant similarities, for example, in the organization of the picornavirus and flavivirus genomes and of the rhabdovirus and paramyxovirus genomes. **Genomics**, the elucidation of evolutionary relationships by analyses of nucleic acid and protein sequence similarities, increasingly is being used to order members within a virus family, to classify newly isolated viral nucleic acids, and to predict the functions of genes. For example, human herpesvirus 8 was placed in the subfamily *Gammaherpesvirinae* on the basis of sequence analysis of a small segment of its DNA, and hepatitis C virus was classified as a member of the family *Flaviviridae* from the sequence of a cloned DNA copy of its genome. Indeed, as our knowledge of molecular properties of viruses and their replication has increased, it has become apparent that *any* two-dimensional comparison (e.g., virus versus size, or virus versus capsid morphology) is somewhat misleading. For example, *Hepadnaviridae*, *Retroviridae*, and some plant viruses are classified as different families on the basis of the nature of their genomes, but all use reverse transcription in their reproductive cycles. Moreover, the viral polymerases that perform this task exhibit similarities in amino acid sequence.

As of the latest report (1995) of the International Committee on Taxonomy of Viruses (ICTV) approximately

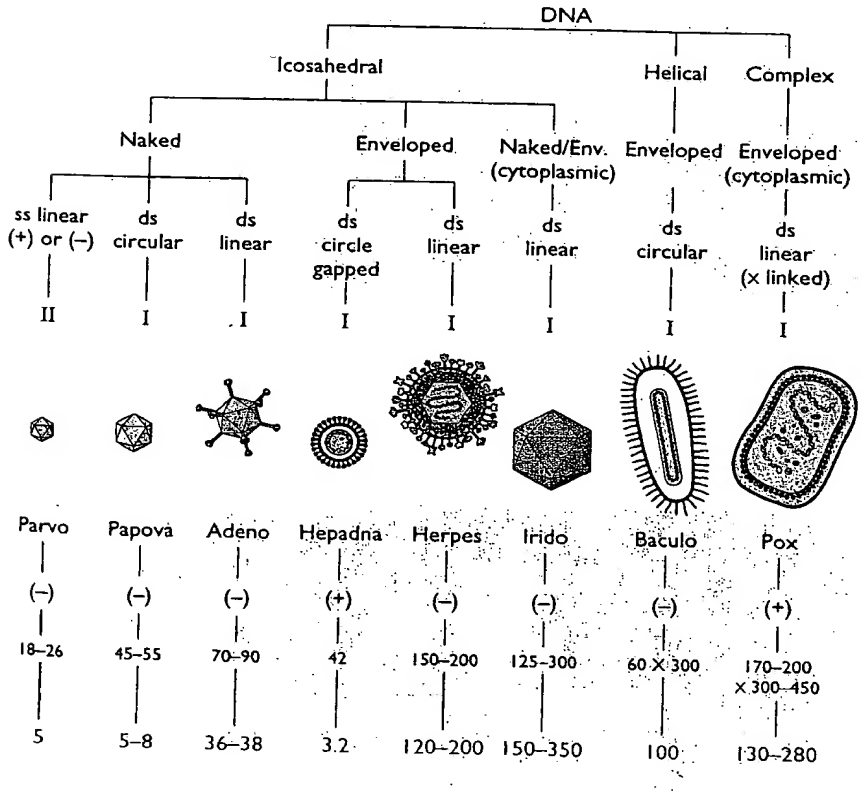

Figure 1.9 Classification schemes for animal viruses. Summary of the major characteristics of 21 representative families of viruses that infect vertebrates and 1 that infects insects. Not all virus families are shown in the figure; the one insect virus family (*Baculoviridae*) is included because it has become an important tool in biotechnology. Adapted from G. P. Martelli et al. (ed.), *Virus Taxonomy Classification and Nomenclature of Viruses: Sixth Report of the International Committee on Taxonomy of Viruses* (Springer-Verlag, Vienna, Austria, 1995).

Biochemistry and structure of PrP^{C} and PrP^{Sc}

Detlev Riesner

Institut für Physikalische Biologie, Heinrich-Heine-Universität Düsseldorf, Düsseldorf, Germany

In a brief historical description, it is shown that the prion model was developed from the biochemical and biophysical properties of the scrapie infectious agent. The biochemical properties of the prion protein which is the major, if not only, component of the prion are outlined in detail. PrP is a host-encoded protein which exists as PrP^{C} (cellular) in the non-infected host, and as PrP^{Sc} (scrapie) as the major component of the scrapie infectious agent. An overview of the purification techniques is given. Although chemically identical, the biophysical features of PrP^{Sc} are drastically different in respect to solubility, structure, and stability; furthermore, specific lipids and a polyglucose scaffold were found in prions, whereas for nucleic acids their absence could be proven. The structure of recombinant PrP in solution is known from spectroscopic studies and with high resolution from NMR analysis. Structural models of PrP^{Sc} were derived recently from electron microscopic analysis of two-dimensional crystals. Conformational transitions of PrP *in vitro* were studied with different techniques in order to mimic the natural PrP^{C} to PrP^{Sc} conversion. Spontaneous transitions can be induced by solvent changes, but at present infectivity cannot be induced *in vitro*.

The early history of the prion model is the history of the biochemical and biophysical properties of the scrapie infectious agent. In searching for a virus, no viral features were found; however, highly enigmatic properties of the infectious agent were demonstrated, such as absence of particles in the electron microscope, no immune response during the infection, and high resistance of the agent against chemical and physical treatment. As early as 1966 from inactivation studies using ionising and UV-irradiation, Alper *et al*[1] concluded that the target size of the scrapie infectious agent (50–150 kDa) is too small for a virus but more characteristic of a protein. Many experimental results were left unexplained until Prusiner took up the inactivation studies and performed systematic analysis using not only chemical and physical, but also enzymatic procedures. He summarized the results under two groups: (i) procedures which modify or destroy nucleic acids do not inactivate scrapie infectivity; and (ii) procedures which modify or destroy proteins inactivate the infectivity. From that, he came to the conclusion that the scrapie infectious agent could not be a virus but a novel

Correspondence to: Prof. Dr Detlev Riesner, Institut für Physikalische Biologie, Heinrich-Heine-Universität Düsseldorf, Universitäts Strasse 1, 40225 Düsseldorf, Germany

N.B. Colour figures are referred to as 'Plates' and appear in a 'Colour plate section' at the front of this volume

British Medical Bulletin 2003; 66: 21–33
DOI 10.1093/bmb/dg66.021

proteinaceous type of an agent, which he termed 'prion' (proteinaceous infectious particle)[2].

To confirm a protein-like agent, the protein (one or more molecular species) had to be purified and characterized. A hydrophobic and, in mild detergents, insoluble protein of molecular weight 33–35 kDa could be highly enriched. In a collaborative research project involving the laboratories of Prusiner, Hood and Weissmann using the Syrian hamster as the experimental animal, the sequence of a peptide fragment was found; from this, the DNA-sequence was determined, first in a cDNA-library and later in a genomic library. The major component of the prion was shown to be a host-encoded protein, later called prion protein[3,4]. In one sense, the finding raised doubts about the prion model, because no foreign information, even a foreign protein, was found; alternatively, it supported the possibility, which indeed was mentioned earlier as a purely theoretical possibility[5], that rather than a self-replicating protein, an infection-induced synthesis of a host protein might be the basis for prion amplification.

The strong, but not complete, resistance of prions to degradation by proteinase K (and other proteases) had supported the hypothesis of prions. When, however, the prion protein was identified as encoded in the host genome, the protein was found also in the non-infected host[6]. Its resistance against proteinase K digestion was barely measurable, so that a clear biochemical distinction between two isoforms of the prion protein could be drawn: the cellular prion protein PrP^{C} in the non-infected organism, and the scrapie isoform PrP^{Sc} as the major component of the purified infectious agent. It should be emphasized that proteinase K resistance of PrP was used as a biochemical marker for infectivity, and often 'PrP^{Sc}' and 'PrPres' (for resistance) were used synonymously. Later, however, it was shown, that infectivity and proteinase K resistance do not correlate in all cases; therefore, in this chapter, PrP^{Sc} is used for the property of infectivity and PrPres for proteinase K resistance, respectively.

Chemical properties of PrP and recombinant PrP

A few biochemical features of PrP were the basis of the prion hypothesis in the early days. In the mean time, PrP is one of the most intensively studied proteins, its chemical properties are well known whereas the biological function of PrP^{C} is still under discussion as outlined elsewhere in this volume.

Plate I summarizes the amino acid sequence, processing, and post-translational modifications of PrP from the hamster. The final, processed form of PrP contains amino acids 23–231 from the original translation product of 253 amino acids. Peptide 1–22 is cleaved as signal peptide during trafficking,

and peptide 232–253 is replaced by the glycosyl-phosphatidylinositol-anchor (for details see elsewhere in this volume). The cellular form is attached *via* the anchor to the outer membrane. Asparagine residues 181 and 197 carry highly branched glycosyl groups with sialic acid substitutions. PrP is always isolated as a mixture of three forms – unglycosylated, with one glycosyl-, and with two glycosyl-groups. A disulphide bridge is formed between Cys179 and Cys214. As indicated in Plate I, PrP contains 2 hexarepeats and 5 octarepeats in its N-terminus (see Prusiner[7] and Weissmann[8]).

The amino acid sequence is the same whether derived from the genomic DNA sequence or directly by peptide sequencing. PrP^c and PrP^{Sc} are identical with respect to all chemical features described in Plate I. Note, however, that the glycosyl groups are heterogeneous, and only typical glycosyl groups are depicted in Plate I. Since it is nearly impossible to compare quantitatively distributions of different glycosyl groups, the chemical identity of PrP^c and PrP^{Sc} is not completely safe in this respect.

Purification of PrP was attempted first in efforts to purify the infectious agent from the brain of infected animals. This became possible only after the hamster was introduced as experimental animal where there is a relatively short incubation time of 3–5 months instead of one or more years in the case of mouse or sheep. Furthermore, in the hamster the infectious dose (ID_{50}) could be determined not only by end-point titration using about 50 animals for one value, but also by the incubation time assay[9] in 4–6 hamsters. The purification procedure consists of a homogenization of the tissue and a series of precipitations and differential centrifugations. In the standard procedure, the solvent contains detergents, and a protein digestion step with proteinase K is included. Thus, the proteinase K resistance of PrP^{Sc} was essential for the purification, and PrP 27–30 was obtained as the purified product[10]. The criteria for optimization are the total yield of infectivity and the specific infectivity (*i.e.* ID_{50}/g of material).

Besides the need for PrP^{Sc} purification, for many studies purified PrP^c is also required. Although the amount of PrP^c in brain is very high in contrast to other tissues, it represents less than 0.1% of the total central nervous system proteins. For example, from 100 hamster brains only a few micrograms of purified PrP^c were obtained in an optimal procedure.

Obviously, expression of recombinant PrP in *Escherichia coli* was required. First attempts to isolate PrP from *E. coli* yielded either low expression levels or low purification efficiency because of the instability and insolubility of the protein. Furthermore, the disulphide bond in PrP, which is essential for correct folding of PrP, is not formed under the reducing conditions in the cytoplasm of *E. coli*. Attempts to fuse PrP with proteins that target the product in the periplasm and thereby spontaneously form the disulphide bond *in vivo* were not effective in

producing larger quantities of PrP. Therefore, recombinant PrP was purified and afterwards reconstituted by denaturing under harsh conditions (8 M urea or 5 M guanidinium hydrochloride), the disulphide bond was formed under oxidizing conditions, and than PrP was renatured by dialysing out the denaturant[11]. This strategy is now used for the purification of recombinant PrP in high amounts.

Eukaryotic expression systems are of particular interest because they yield post-translationally modified PrP, *i.e.* a PrP which is very similar or identical with PrP^C. Many eukaryotic cell systems including those of yeast and mammals were tested for expression of PrP. However, in most of these cases, difficulties occurred (unstable transfection, low levels of expression, insolubility of the protein, or difficulties in purifying PrP) and prevented those procedures becoming standard.

Finally, a transgenic mammalian cell system of Chinese hamster ovary (CHO) cells was established that generated PrP^C at high levels of expression (~14-fold higher than in hamster brain). By this method, purified PrP^C in amounts of 10–100 μg can be prepared[12]. Although this yield is still rather low in comparison to the yield of recombinant PrP purified from *E. coli* cells, purified PrP^C is now available in amounts sufficient for some biophysical studies.

Chemical properties of PrP^{Sc}

Purified prions, either in the form of 'full-length' PrP^{Sc} or as PrP 27–30, are insoluble, even in mild detergents. In electron micrographs, fibrillar structures also called prion rods are visible (Fig. 1). After staining with

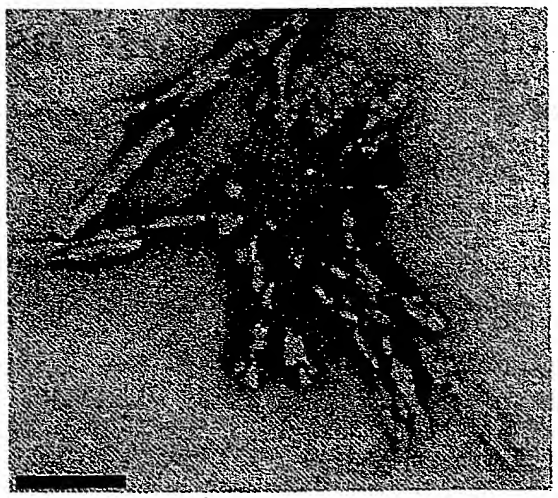

Fig. 1 Prion rods. As obtained from a purification procedure including detergents and proteinase K-treatment.

Congo Red, they show the typical fluorescence birefringence of amyloids[13]. Similar structures were detected in thin sections of the brain of infected animals, which were called originally scrapie associated fibrils (SAF)[14]. It should be noted that, in the brains of CJD or Kuru victims, PrP deposits can be detected as diffuse deposits, amyloidic fibres, condensed plaques, or florid plaques.

The high tendency to aggregate correlates with a PrP^{Sc}-specific resistance against digestion with proteinase K. In Plate II, the Western blot of an SDS-gel electrophoresis of PrP^{C} and PrP^{Sc}, without and with proteinase K digestion, respectively, is depicted. The characteristic three bands of PrP (*i.e.* without, with one and with two glycosyl groups) are visible; they disappear completely after proteinase K digestion of PrP^{C} which results in small peptides. In the case of PrP^{Sc}, however, the bands remain nearly undiminished in intensity although shifted to lower molecular weight. These are the N-terminally truncated forms of PrP^{Sc}, called PrP 27–30. From the right panel of Plate II, it can be seen that the 'full-length'-PrP is cleaved around amino acid 90. The cleavage product (PrP 27–30) is fully infectious and, indeed, it is also the product of the purification procedure described above[10]. Furthermore, it should be noted that all presently available routine tests for BSE and scrapie are based on the proteinase K resistance of PrP 27–30.

The prion model might well be explained on the basis of conformational changes of the prion protein which are induced directly or indirectly by the invading PrP^{Sc}. The phenomenon of prion strains, however, is hard to explain in a similar manner. Although different physicochemical properties were found with different prion strains[15], these could not be attributed to different conformations of single PrP molecules but only to the highly aggregated and insoluble PrP. Even if the principal replication features of prions did not depend on nucleic acids, it was argued that at least the strain specificity might be determined by nucleic acid molecules[16]. Many attempts had been undertaken to find nucleic acids, all without success, which did not prove, however, the absence of nucleic acids. One series of studies was arranged in a way that nucleic acids either would have been found or would be excluded as essential components to prion infectivity[17,18]. Using highly purified infectious material, the number of nucleic acid molecules irrespective of their chemical nature and structure but depending on their size were determined quantitatively and related to the number of infectious units. For all nucleic acids larger than about 80 (in later work 50) nucleotides, less than one molecule of nucleic acid was determined per infectious unit. Consequently, infectious units exist without a nucleic acid – and the virus hypothesis was disproven finally with quantitative biophysical methods.

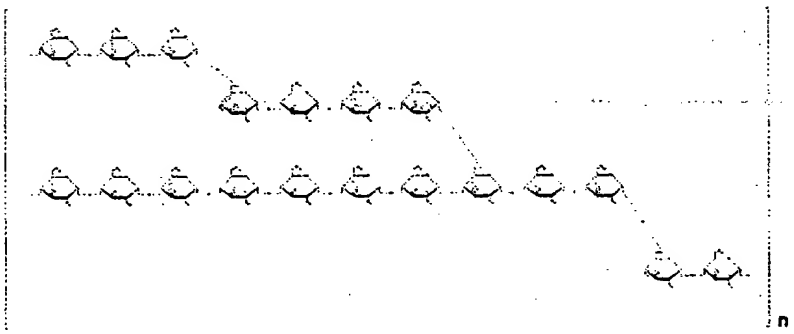

Fig. 2 Schematic presentation of the polyglucose scaffold as found in prion rods. The estimated molecular weight is above 200,000.

The lipophilic nature of highly purified prions suggested that not only a glycolipid anchor is linked to PrP but, in addition, lipids might be associated non-covalently with PrP. A chemical analysis revealed specific lipids which amounted to around 1% of purified prions[19]. These are sphingomyelin, α-hydroxy-cerebroside and cholesterol depending on the method of purification. Both lipids are known to be components of the outside of the cell membrane in caveolae-like sites, where PrP^C also accumulates. It could not be shown that the lipids are essential for infectivity, but their presence in prions might indicate the origin of prions, namely the site of PrP^C accumulation on the outside of the cell membrane.

Early experiments, in which prion rods were digested extensively with proteinase K, had shown that the rod-like structure was maintained in electron micrographs even if PrP was digested by more than 99%[20]. This result had pointed to an additional structural component. It was identified much later as polymeric sugar consisting of α-1,4-linked and 1,4,6-branched polyglucose[21]. Thus, this sugar component is clearly different from the glycosyl groups which are attached covalently to PrP. A schematic presentation is given in Figure 2. Since the polysaccharide amounted to up to 10% (w/w) of highly purified prions, it might be regarded as a structural scaffold contributing to the high chemical and physical stability of prions.

Structure of PrP^C and PrP^{Sc}

It has been indicated above that PrP^C and PrP^{Sc} are different in respect to solubility, fibril formation, proteinase K resistance and other features. These differences could be either a consequence of ligands bound to one

Table 1 Secondary structure of PrP in different isoforms

	α-helix (%)	β-sheet (%)
PrP^{c}	43	–
PrP^{Sc}	20	34
PrP 27–30	29	31

isoform but not to the other or a consequence of a different secondary and tertiary structure of PrP^{C} and PrP^{Sc}, respectively. First indications for clear differences in the secondary structure came from spectroscopic measurements applying circular dichroism and infrared spectroscopy[22,23]. From those measurements, α-helix and β-sheet contents could be determined. The numbers given in Table 1 are not very accurate, since the analysis on PrP^{Sc} had to be carried out on insoluble samples; however, they show clearly that PrP^{C} is dominated by α-helices and has only little β-sheet content, whereas PrP^{Sc}, *i.e.* 'full-length', or PrP 27–30 are characterized by similar amounts of α-helices and β-sheets.

Natural PrP^{C} could not be used to apply NMR spectroscopy or X-ray analysis for determination of the exact three-dimensional structure. The amount of material available was too small, the samples were not sufficiently pure, and the concentration was too low. These three hurdles were only overcome with recombinant PrP. In addition, recombinant PrP was synthesized in a form labelled with ^{15}N or ^{13}C. Even then, it took several years before the groups of Wüthrich[24] and a little later of James[25] analysed the structure of the C-terminal part of PrP, *i.e.* amino acids 121–231. As shown in Plate III for PrP of mouse and of man[26], the structure consists of three α-helices (amino acids 144–154, 175–193 and 200–219) and a small antiparallel β-sheet (amino acids 128–131 and 161–164). When the structure of 'full-length' PrP (*i.e.* amino acids 23–231) was analysed it was evident that the C-terminal part (*i.e.* amino acids 126–231) contained the complete globular part of the structure, whereas the N-terminus (*i.e.* amino acids 23–125) was more or less flexible[27]. Close to the small β-sheet, the disulphide bridge connects helix 2 and helix 3. The region between the β-sheet and helix 2 (amino acids 166–171) could be determined only with less accuracy possibly because of some structural flexibility. This region, however, is of particular functional interest. Different lines of evidence such as antibody binding, transgenic animals with mutations in that region, binding of the hypothetical factor X, *etc.* argue that the species barrier might be localized in that region. Furthermore, the minor differences in the structure of mouse and hamster PrP on the one hand and of bovine[28] and human PrP on the other are restricted to that part of the molecule.

It should be noted that the structure described above is the best description of the PrP^{C} structure presently available, but that it was

obtained from recombinant PrP. The glycosyl-groups of PrP^C probably do not alter the structure significantly, but the fact that PrP^C is attached to the membrane by the glycolipid anchor might have more influence, particularly if one considers the structure of the N-terminus which was found unstructured when free in solution (see above). Furthermore, it is known that the N-terminus and, in particular, the octarepeat of the N-terminus bind 4–6 copper ions in a co-operative manner which definitely would induce more structure than presently known from the NMR analysis.

The NMR-structure of PrP is a monomeric structure. Several reports in the literature indicate that PrP in its α-helical structure can form dimers under physiological or close to physiological conditions[29,30]. Dimers in solution show the intact intramolecular disulphide bridge. Consequently, dimerization is not induced by oxidizing the disulphide bridge and reforming it in an intermolecular structure. The latter situation was, however, found in a recent crystal structure of a dimer of PrP (120–231)[31]; dimers were formed by domain swapping and intermolecular disulphide bridging. Whether this structure is a consequence of the long-time crystallization, or might indicate a physiological state, cannot be stated at present.

As mentioned above, PrP^{Sc} or PrP 27–30 are not accessible to structural analysis by NMR or X-ray analysis because of their insolubility. Attempts were made[32] to use the structure described above as a starting model, change α-helices into β-sheets and, in this way, develop a model for PrP^{Sc}. These models assume that helix 2 and helix 3 are unchanged in accordance with antibody binding data, but they are incomplete in the sense that they are models for isolated molecules whereas PrP^{Sc} as well as PrP 27–30 were found only in aggregated forms. Thus, one has to assume that the PrP^{Sc} structure is stabilized by intermolecular interactions.

A new approach was followed by Wille from Prusiner's laboratory who was able to prepare two-dimensional crystalline-like arrays of PrP^{Sc}- or PrP^{Sc}-like molecules[33]. Those samples were studied by electron microscopy and, because of the crystalline-like arrangement, images could be reconstructed from the repetitive unit with fairly high resolution. A hexagonal symmetry was visible, but it could not be decided whether one unit is built from 3 or 6 molecules. The electron density map could be fitted best if, instead of β-sheets, a β-helix was assumed. The structure of the β-helix type is known from other fibrillar proteins; spectroscopically, β-sheets and β-helices cannot be differentiated, so that the new model would not contradict earlier spectroscopic studies. The model is depicted in Plate 1V. In summary, the β-helical N-terminus is located in the inner part of the hexagonal unit, with the helices 2 and 3 at the outer side and the glycosyl-groups pointing into the space between the hexagonal units. Most probably, the

model shown in Plate IV is not the final description of the structure of PrP^{Sc}, but it is the best model currently available and takes into account both electron microscopic and spectroscopic data as well as the intermolecular stabilization of the PrP^{Sc} structure.

Conformational transitions of PrP *in vitro*

Structural and other chemical and physical properties of PrP^{C} and PrP^{Sc} in the purified state have been described above. PrP^{C} was characterized by α-helical structure, solubility as a monomeric or dimeric molecule, and proteinase K sensitivity. Since no functional test for PrP^{C} is available, it is more accurate to speak about a PrP^{C}-like conformation when the such properties are found. Similarly, for PrP^{Sc}, a β-sheet-rich structure, insoluble aggregates, and proteinase K resistance are typical, but these features are not sufficient for PrP^{Sc}, because PrP^{Sc} stands for infectivity and, presently, the re-establishment of infectivity has not been achieved. Thus, the properties of PrP^{Sc} as mentioned above are those of a PrP^{Sc}-like molecule and do not infer infectivity.

Conformational transitions might be either denaturation processes of PrP^{C} or PrP^{Sc}, transitions between PrP^{C} and PrP^{Sc} induced by varying solvent conditions, or induction of the PrP^{C} to PrP^{Sc} transition by an existing seed of PrP^{Sc} (as described in detail elsewhere in this volume).

The denaturation of the globular domain of recombinant PrP (121–231) by addition of up to 8 M urea was analyzed quantitatively by recording the ellipticity at 222 nm[34]. One co-operative transition was obtained at pH 7.0 with a free energy of –28.6 kJ/mol for structure formation. At pH 4.0, an intermediate state could be identified with lowered α-helicity and increased β-sheet content; at present, it cannot be decided whether the intermediate would also be an intermediate on the pathway to PrP^{Sc}-like conformations. From the reversibility of the denaturation process, it was concluded that the PrP^{C}-like conformation is the state of lowest free energy in buffer without detergent. This conclusion might be restricted, however, to the fragment PrP (121–231).

Similar experiments, but also taking into account the mechanism of refolding by kinetic analysis, were carried out on recombinant PrP (89–231) from mouse which is the recombinant equivalent of PrP 27–30[35]. In this fragment, β-sheet-rich oligomers and even fibrils were formed at pH 3.6. However, after switching from the fully denaturing conditions of 10 M urea to native conditions without urea, first the monomeric α-helical conformation and from that (in a very slow process of hours or even days) β-sheet oligomers and finally fibrils were formed. The presence of urea during the incubation speeded up the formation of the β-sheet-rich conformation, and the presence of 5 M urea directly

induced formation of β-sheet-rich oligomers without running through the α-helical state. Consequently, at acidic pH, folding of PrP to the α-helical state is under kinetic control and the thermodynamically stable state is the β-sheet rich state.

More close to the natural conditions of the PrP^{C} to PrP^{Sc} transition were experiments in which the PrP^{C}-like, α-helical state was established first as it is in the non-infected organism[36]. Then the transition to the PrP^{Sc}-like conformation was induced by slightly denaturing conditions, (*e.g.* 1 M guanidinium hydrochloride). Also, these experiments were carried out at acidic pH (4.0), and the conversion process could be induced by a wide variety of conditions combining mild denaturants and different salts. In accordance with renaturation experiments (see above), it was found that β-sheet formation is always connected with aggregation and that the most stable state, at least at acidic pH, is the β-sheet-rich aggregated state. An exception was shown under conditions reducing the disulphide bridge; it was reported that acidic and reducing conditions could induce a β-sheet-rich and monomeric state[37]. It is not known whether this finding is relevant to PrP^{C} to PrP^{Sc} conversion in nature because the intramolecular disulphide bridge is present in both states and in all other conversion experiments the disulphide bridge was not opened transiently[38].

The earliest studies on the *in vitro* conversion were carried out with natural PrP and at neutral pH[39]. Infectious PrP 27–30 was converted to an α-helical, oligomeric and non-infectious form by addition of 0.3% sodium-dodecylsulphate (SDS). Further addition of 30% acetonitrile or mere dilution of SDS to 0.01%[40], re-established a β-sheet-rich, aggregated and partially proteinase K-resistant conformation. Although natural PrP was used which was infectious before the conversion, infectivity could not be re-established. These experiments were closest to natural conditions if the low concentrations of SDS were regarded as a membrane-like environment. It was also shown that the conversion occurs in steps, first fast formation of β-sheet structure concomitant with forming small oligomers, then larger oligomers in minutes to an hour, and finally large insoluble aggregates in hours to days. Applying the same conversion system to recombinant PrP (90–231), systematic studies of the influence of varying SDS concentrations were carried out and several intermediate states described (Fig. 3)[30]. In 0.06–0.1% SDS, an α-helical dimer is present as a thermodynamically stable state which is converted in a co-operative manner in 0.04–0.06% SDS to a β-sheet-rich oligomeric state. As recently determined (Nagel-Steger *et al*, unpublished), the oligomeric state with 12–16 molecules is of particular interest for further biophysical studies since it is stable in solution. In low SDS concentrations (< 0.02% SDS), large insoluble aggregates (see above) are formed which also remain stable after the SDS has been

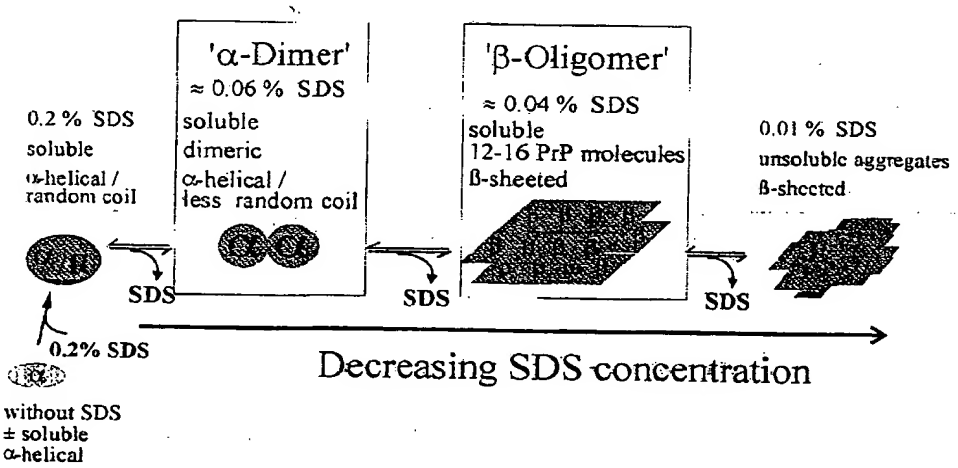

Fig. 3 Intermediates in the *in vitro* conversion of recombinant PrP (90–231).

washed out completely. In buffer without detergent at pH 7, the PrP^{C}-like as well as the PrP^{Sc}-like conformations can be established, but the stable state is the PrP^{Sc}-like conformation, and the conversion can be induced by different detergents, even in very low concentrations (see also Xiong *et al*[41]).

Conclusions

What is the conclusion from all the *in vitro* conversion studies? Evidently, the thermodynamically stable state is the PrP^{Sc}-like state, and this would be true for lysosomal acidic pH or the cell-surface neutral pH. A high activation barrier renders the transition very slow (*i.e.* hours, days or even weeks). Formation of the β-sheet-rich structure is always correlated with oligomerization at least if the naturally occurring disulphide bridge is intact. Whether β-sheet oligomers are intermediates on the pathway to PrP^{Sc} or a dead-end product is at present an artificial discussion because the PrP^{Sc}-like state as available is not infectious and a final decision on the right pathway cannot be made. If the PrP^{C}-conformation is not the thermodynamically stable state, but only metastable, the question remains why a transition to PrP^{Sc} does not occur much more frequently in nature as a spontaneous transition. It is, however, not a discrepancy if one takes into account that PrP^{C} is anchored in the lipid membrane, and all studies described were carried out in aqueous buffer. Consequently, as an additional transition of PrP^{C}, one has to include the distribution between the aqueous and the lipid

phase which would definitely stabilize PrP^C in nature to prevent a spontaneous transition.

Acknowledgement

The author thanks his co-workers E Birkmann, C Dumpitak, K Elfrink, H Gruber, and Drs K Jansen and J Schell for their help in preparing the manuscript.

References

1 Alper T, Haig DA, Clarke MC. The exceptionally small size of the scrapie agent. *Biochem Biophys Res Commun* 1966; 22: 278–84
2 Prusiner SB. Novel proteinaceous infectious particles cause scrapie. *Science* 1982; 216: 136–44
3 Oesch B, Westaway D, Walchli M *et al.* A cellular gene encodes scrapie PrP 27–30 protein. *Cell* 1985; 40: 735–46
4 Basler K, Oesch B, Scott M *et al.* Scrapie and cellular PrP isoforms are encoded by the same chromosomal gene. *Cell* 1986; 46: 417–28
5 Griffith JS. Self-replication and scrapie. *Nature* 1967; 215: 1043–4
6 Barry RA, Kent SB, McKinley MP *et al.* Scrapie and cellular prion proteins share polypeptide epitopes. *J Infect Dis* 1986; 153: 848–54
7 Prusiner SB. Scrapie prions. *Annu Rev Microbiol* 1989; 43: 345–74
8 Weissmann C. Molecular biology of prion diseases. *Trends Cell Biol* 1994; 4: 10–4
9 Prusiner SB, Cochran SP, Groth DF, Downey DE, Bowman KA, Martinez HM. Measurement of the scrapie agent using an incubation time interval assay. *Ann Neurol* 1982; 11: 353–8
10 McKinley MP, Meyer RK, Kenaga L *et al.* Scrapie prion rod formation *in vitro* requires both detergent extraction and limited proteolysis. *J Virol* 1991; 65: 1340–51
11 Mehlhorn I, Groth D, Stockel J *et al.* High-level expression and characterization of a purified 142-residue polypeptide of the prion protein. *Biochemistry* 1996; 35: 5528–37
12 Blochberger TC, Cooper C, Peretz D *et al.* Prion protein expression in Chinese hamster ovary cells using a glutamine synthetase selection and amplification system. *Protein Eng* 1997; 10: 1465–73
13 Prusiner SB, McKinley MP, Bowman KA *et al.* Scrapie prions aggregate to form amyloid-like birefringent rods. *Cell* 1983; 35: 349–58
14 Merz PA, Somerville RA, Wisniewski HM, Iqbal K. Abnormal fibrils from scrapie-infected brain. *Acta Neuropathol* 1981; 54: 63–74
15 Safar J, Wille H, Itri V *et al.* Eight prion strains have PrP(Sc) molecules with different conformations. *Nat Med* 1998; 4: 1157–65
16 Weissmann C. A 'unified theory' of prion propagation. *Nature* 1991; 352: 679–83
17 Meyer N, Rosenbaum V, Schmidt B *et al.* Search for a putative scrapie genome in purified prion fractions reveals a paucity of nucleic acids. *J Gen Virol* 1991; 72: 37–49
18 Kellings K, Meyer N, Mirenda C, Prusiner SB, Riesner D. Further analysis of nucleic acids in purified scrapie prion preparations by improved return refocusing gel electrophoresis (RRGE). *J Gen Virol* 1992; 73: 1025–9
19 Klein TR, Kirsch D, Kaufmann R, Riesner D. Prion rods contain small amounts of two host sphingolipids as revealed by thin-layer chromatography and mass spectrometry. *Biol Chem* 1998; 379: 655–66
20 McKinley MP, Braunfeld MB, Bellinger CG, Prusiner SB. Molecular characteristic of prion rods purified from scrapie-infected hamster brain. *J Infect Dis* 1986; 154: 110–20
21 Appel TR, Dumpitak Ch, Mathiesen U, Riesner D. Prion rods contain an inert polysaccharide scaffold. *Biol Chem* 1999; 380: 1295–306

22 Caughey BW, Dong A, Bhat KS, Ernst D, Hayes SF, Caughey WS. Secondary structure analysis of the scrapie-associated protein PrP (27–30) in water by infrared spectroscopy. *Biochemistry* 1991; 30: 7672–80

23 Safar J, Roller PP, Gajdusek DC, Gibbs Jr CJ. Conformational transitions, dissociation, and unfolding of scrapie amyloid (prion) protein. *J Biol Chem* 1993; 268: 20276–84

24 Riek R, Hornemann S, Wider G, Billeter M, Glockshuber R, Wuthrich K. NMR structure of the mouse prion protein domain PrP(121–321). *Nature* 1996; 382: 180–2

25 James TL, Liu H, Ulyanov NB *et al.* Solution structure of a 142-residue recombinant prion protein corresponding to the infectious fragment of the scrapie isoform. *Proc Natl Acad Sci USA* 1997; 94: 10086–91

26 Zahn R, Liu A, Lührs T *et al.* NMR solution structure of the human prion protein. *Proc Natl Acad Sci USA* 2000; 97: 145–50

27 Riek R, Hornemann S, Wider G, Glockshuber R, Wüthrich K. NMR characterization of the full-length recombinant murine prion protein, mPrP(23–231). *FEBS Lett* 1997; 413: 282–8

28 Garcia FL, Zahn R, Riek R, Wüthrich K. NMR structure of the bovine prion protein. *Proc Natl Acad Sci USA* 2000; 97: 8334–9

29 Meyer RK, Lustig A, Oesch B, Fatzer R, Zurbriggen A, Vandeveld M. A monomer–dimer equilibrium of a cellular prion protein (PrP^C) not observed with recombinant PrP. *J Biol Chem* 2000; 275: 38081–7

30 Jansen K, Schäfer O, Birkmann E *et al.* Structural intermediates in the putative pathway from the cellular prion protein to the pathogenic form. *Biol Chem* 2001; 382: 683–91

31 Knaus KJ, Morillas M, Swietnicki W, Malone M, Surewicz WK, Yee VC. Crystal structure of the human prion protein reveals a mechanism for oligomerization. *Nat Struct Biol* 2001; 8: 770–4

32 Pan KM, Baldwin M, Nguyen J *et al.* Conversion of alpha-helices into beta-sheets features in the formation of the scrapie prion protein. *Proc Natl Acad Sci USA* 1993; 90: 10962–6

33 Wille H, Michelitsch MD, Guénebaut V *et al.* Structural studies of the scrapie prion protein by electron crystallography. *Proc Natl Acad Sci USA* 2002; 99: 3563–8

34 Hornemann S, Glockshuber R. A scrapie-like unfolding intermediate of the prion protein domain PrP(121–231) induced by acidic pH. *Proc Natl Acad Sci USA* 1998; 95: 6010–4

35 Baskakov IV, Legname G, Prusiner SB, Cohen FE. Folding of prion protein to its native α-helical conformation is under kinetic control. *J Biol Chem* 2001; 276: 19687–90

36 Morillas M, Swietnicki W, Gambetti P, Surewicz WK. Membrane environment alters the conformational structure of the recombinant human prion protein. *J Biol Chem* 1999; 274: 36859–65

37 Jackson GS, Hosszu LLP, Power A *et al.* Reversible conversion of monomeric human prion protein between native and fibrilogenic conformations. *Science* 1999; 283: 1935–7

38 Welker E, Raymond LD, Scheraga HA, Caughey B. Intramolecular versus intermolecular disulfide bonds in prion proteins. *J Biol Chem* 2002; 277: 33477–81

39 Riesner D, Kellings K, Post K *et al.* Disruption of prion rods generates spherical particles composed of four to six PrP 27–30 molecules that have a high α-helical content and are non-infectious. *J Virol* 1996; 70: 1714–22

40 Post K, Pitschke M, Schäfer O *et al.* Rapid acquisition of β-sheet structure in the prion protein prior to multimer formation. *Biol Chem* 1998; 379: 1307–17

41 Xiong L-W, Raymond LD, Hayes SF, Raymond GJ, Caughey B. Conformational change, aggregation and fibril formation induced by detergent treatments of cellular prion protein. *J Neurochem* 2001; 79: 669–78